accepted for publication in J. Atmos. Solar-Terr. Phys. (18 Feb 2010)

Statistical properties of nonlinear wave signatures in OH and O_2 airglow brightness data observed at lower midlatitudes

Jürgen Scheer, Esteban R. Reisin
Instituto de Astronomía y Física del Espacio (CONICET-UBA), C.C. 67, Suc. 28, 1428, Buenos Aires, Argentina

Abstract: Among 2187 nights of airglow observations of the OH(6-2) and O_2b(0-1) bands from Argentina (mainly from El Leoncito, 32°S 69°W), 132 show airglow brightness jumps (ABJs) of short duration (16 minutes median). ABJs are supposed to be related to mesospheric bores or similar nonlinear waves. Several occurrence patterns were identified, which a successful explanation must take into account. ABJs occur preferably in the OH layer at 87 km, and are less likely in the O_2 layer at 95 km, maybe because ducts prefer lower altitudes. The seasonal distribution of nights when ABJs are observed only in the OH layer clearly shows a winter maximum centered around solstice, and equinox minima. In contrast, the seasonal distribution of ABJ nights in O_2 is flat. Most ABJs simultaneously present in OH and O_2 show anticorrelated variation between both layers. ABJ nights tend to occur in clusters lasting several days, which probably reflects duct lifetime.

Keywords: mesopause region airglow; mesospheric bores; solitary waves; ducting conditions

1. Introduction

The term "nonlinear waves" is occasionally used in the aeronomic literature for internal waves whose amplitudes grow so large by propagating upward in the atmosphere that deviations from linear wave theory become non-negligible. A particularly clear discussion of how wave momentum is deposited into the mean flow, avoiding the critical-level singularity of the linear theory, but also without wave breaking, was the early theoretical study by Mobbs (1985, and references to part I and II therein). We here use the term in a different sense, namely for waves which persist in spite of their very large amplitude.

Signatures of such nonlinear waves are so different from the appearance of normal (linear, or quasi-linear) gravity waves, that they have immediately aroused the attention of investigators. The first observations of nonlinear waves in the mesopause region seem to have been during the ALOHA campaign of 1993. Bore and wall events were distinguished (Taylor et al., 1995; Swenson et al., 1998). The first simple model designed to explain the observations by Taylor et al. (1995) in terms of a nonlinear wave ducted in a waveguide channel (in analogy to a tidal river bore) was published by Dewan and Picard (1998). The history of observations of similar events

and the different attempted explanations have been reviewed by Brown et al. (2004). More recent observations were reported by She et al. (2004), Fechine et al. (2005; 2009), Medeiros et al. (2005), Smith et al. (2005; 2006), Nielsen et al. (2006), Shiokawa et al. (2006), Li et al. (2007), Snively et al. (2007), Bageston et al. (2009), and Yue et al. (2009).

The general concept of the Dewan and Picard (1998) model was applied by Seyler (2005) to further elaborate on the study of bore formation in an idealized atmosphere under different sets of scale parameters. Laughman et al. (2009) used their own model, similarly based on the incompressible Navier-Stokes equations, to simulate the effect of thermal ducts, Doppler ducts, and a combination of the two. Both models have been able to reproduce solitary waves with steep horizontal gradients similar to the ALOHA-93 observations. Solitary waves are solutions of nonlinear wave equations like the Korteweg-de-Vries or Benjamin-Ono equations (e.g., Drazin and Johnson, 1993). The development of bores shown in Fig. 6 of Seyler (2005) and Fig. 4 of Laughman et al. (2009) is similar to the animation for a solution of the Korteweg-de-Vries equation (with a sine function as initial condition, and periodic boundaries) at K. Takasaki's web site http://www.math.h.kyoto-u.ac.jp/~takasaki/soliton-lab/gallery/solitons/kdv-sin-a.gif. It is convenient to extend the term "solitary wave" to include such temporally changing phenomena, and not limit it to structures of constant shape.

According to some theories that describe the reaction of airglow layers to the passage of atmospheric waves (e.g., Tarasick and Hines, 1990; Swenson and Gardner, 1998; Liu and Swenson, 2003; for comparison with observations, see also Reisin and Scheer, 1996), any type of wave signature should also manifest itself as a temperature variation, for being similarly subject to dynamical forcing. However, as expressed by Krassovsky's ratio, relative (band integrated) airglow brightness variations can be expected to be greater than relative temperature variations, by factors between two and an order of magnitude (Reisin and Scheer, 1996; 2001), and therefore easier to detect. This is probably the reason why reports of unusual wave features in the literature have mostly been based on monitoring airglow brightness variations, especially with airglow imagers, rather than on temperature variations. Different airglow emissions (OH, O_2, Na, and OI green line) can be used to observe wave structure at different altitudes in the mesopause region.

Most of the reports published so far deal with only one or a few nonlinear wave observations. An exception are the occurrence statistics published by Fechine et al. (2005) and by Medeiros et al. (2005) based on 64 bore events observed at an equatorial site in Brazil.

Almost all the previous observations have been done with airglow imagers, occasionally complemented by other instrumentation to permit a better identification

of the nonlinear wave (e.g., Smith et al., 2003; Li et al., 2007). At a fixed point in the sky, the passage of such a wave appears as a change in airglow brightness, as can be observed by airglow photometers or spectrometers. This airglow brightness change may be so dramatic that it can be clearly distinguished from any ordinary intensity oscillation due to linear waves. Such was the case with two events observed by the Argentine airglow spectrometer in combination with an imager, in August 2001 (Smith et al., 2006). For lack of an established term, the phenomenon as observed by an airglow spectrometer may be called "airglow brightness jump" (abbreviated as ABJ). We assume that ABJs are valid proxies for nonlinear wave events, suitable for their identification even in the absence of information about horizontal structure, which would permit a further classification.

In this paper, we describe the statistical characteristics, including the seasonal distribution, of nights which exhibit ABJ signatures. We will show that the results depend strongly on altitude, making use of our observations of the OH or O_2 airglow emissions that are routinely obtained from our airglow spectrometer at lower midlatitudes (mostly at El Leoncito, 31.8°S, 69.2°W).

2. Instrumentation, data, and analysis

The observations reported here were done with the zenith-looking Argentine Airglow Spectrometer with a small field of view (0.4° x 2°). The instrument gives time series of band-integrated airglow brightness of the OH(6-2) and O_2(0-1) airglow emissions and the rotational temperatures corresponding to the nominal heights of 87 and 95 km, respectively. For an update on instrumentation and data analysis, see Scheer and Reisin (2001, and references therein). The data here used are from campaigns in 1986, 1987, 1988, 1992, and 1997, and from quasi-continuous observations since April 1998 until early 2003, and from 2006 to mid-December of 2008. For the data before 1997, time resolution was 103 s and then improved to 80 s. Except for the short campaign at Buenos Aires (34.6°S, 58.4°W) in 1988, the observations were done from the astronomical site El Leoncito (31.8°S, 69.2°W). See Table 1 for an overview of the number of nights with data per month in the different years. All months are documented by at least 130 nights of observation (in summer), up to more than 210 (in August and October). This ensures good statistics throughout the seasonal cycle.

In the present context, three instrument characteristics are most relevant for data quality: One is short-term stability, due to the optical and mechanical stability of the tilting interference filter principle, and operation in photon counting mode. The second one is sufficient time resolution to document rapid changes with many data points. Here, the small field of view which corresponds to 0.6 km x 3 km at the emission heights avoids ABJ degradation during the passage of the wave front. The third one is the good immunity against absorption artifacts. This results from the

existence of three independent intensity channels (for OH, O_2, and spectral background). Signal variations due to cloud absorption clearly manifest themselves by simultaneous changes in these three parameters and are therefore easily removed from the airglow channels. With moonlight, cloud effects are even more conspicuous and can be identified from the background signal alone.

Table 1: Number of nights with data for each month in the different years that comprise the data set used, including the total numbers by year and by month.

year	jan	feb	mar	apr	may	jun	jul	aug	sep	oct	nov	dec	sum
1986						5	14			6	10		35
1987									17				17
1988												5	5
1992										16			16
1997								23	21	6	13	9	72
1998	8	1		23	17	26	18	25	9	25	26	14	192
1999	15	12	17	20	9	29	28	11	12	17	21	10	201
2000	15	17	20	20	25	15	14	23	18	26	16	17	226
2001	22	20	16	23	23	11		24	14	24	10	10	197
2002	22	10	22	19	15	27	29	31	30	28	18	29	280
2003	12												12
2006		22	27	30	31	30	25	24	29	31	23	15	287
2007	9	22	31	29	29	29	30	28	23	31	19	31	311
2008	28	29	27	30	29	29	31	30	30	31	29	13	336
sum:	131	133	160	194	178	201	189	219	203	241	185	153	2187

To find ABJs, we use computer-aided visual inspection of the time series of OH and O_2 variations of all the 2187 nights of Table 1. Thereby, the absence of absorption artifacts can be verified and it is easy to extract quantitative information on the events (see below). Some characteristic examples of nights with ABJs (corresponding to different years and months) are shown in Fig. 1. It is not necessary to identify each event in the figure, because they stand out clearly enough. Two of these nights involve OH brightness and temperature (a and d), while the rest only involve brightness (b and c, in OH; e, in O_2; f, in OH and O_2).

Our identification of an ABJ event is based on two criteria, namely, that there is a considerable intensity variation, and that it occurs in a short time. In order to permit a quantitative ranking of the ABJ events for a more objective statistical analysis, the strength and duration of the brightness change is determined. We define the strength of the variation as 2 * |B1 - B2| / (B1 + B2), where the airglow brightness B1 and B2 refers to the beginning and the end of the event. ABJ events can also be ranked in terms of the rate of variation, i.e., strength divided by duration. How start and end of the ABJ are exactly assigned is not very critical for rate, by affecting duration and strength in the same sense. Of course, the statistical homogeneity of the ABJ list must be verified, as will be explained in section 3.

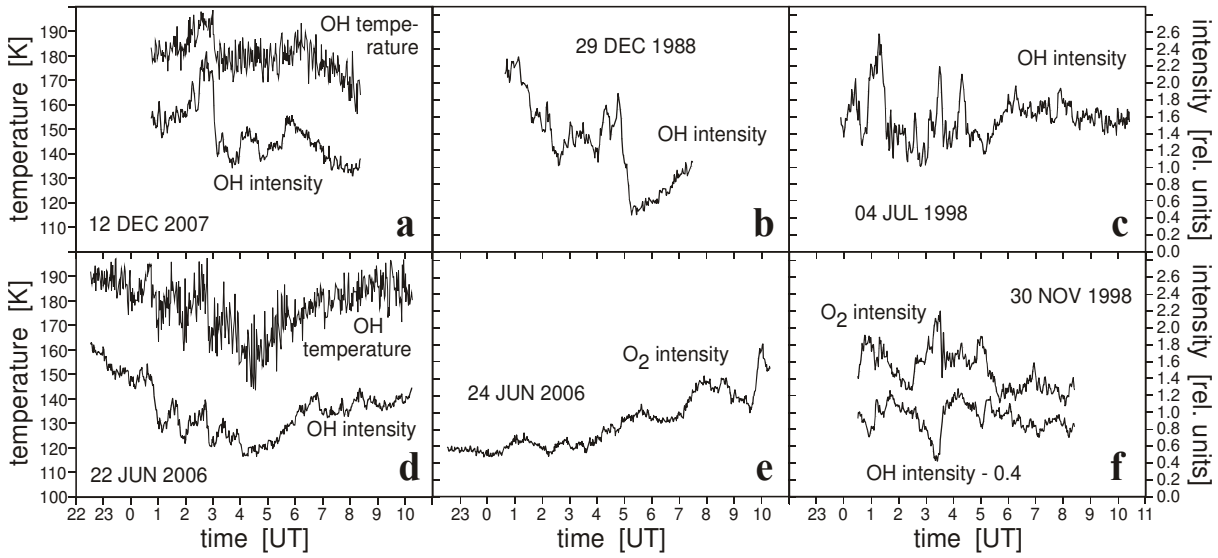

Fig. 1. Nocturnal variations for 6 sample nights showing one or several airglow brightness jumps. Corresponding dates and parameters involved are indicated in each panel. Airglow brightness is expressed as relative intensity units normalized by the long-term mean. Note that the curve for OH intensity in panel (f) is shifted downward by 0.4 units to avoid overlap with the O_2 curve.

We have found 176 ABJ events in 132 nights. When ranked in terms of the strength of the variation, the list starts with nine cases with variations of 125% to 87% , mostly lasting about half an hour. When sorted with respect to event duration, the 9 shortest events last between 4 and 5.5 min (with brightness variations between 32% and 75%). Similarly, the ranking of the rate of variation peaks with values of 9 to 14%/min. Median variation of all events is 52%, median duration 16 min, and median rate of variation 2.7%/min. The three rankings do not exhibit significant gaps, except between some of the greatest values. There are only 3 ABJs lasting more than one hour (62 to 75 min), but they deserve to be included because of their strengths (68% to 85%). The ten weakest cases of the ABJ distribution range between 22% and 32%.

In this statistical context, we now return to our description of Fig. 1. The strong OH brightness drop (by 62%) that stands out in panel a and lasts 12 min is accompanied by a 15 K temperature decrease. The ratio of the corresponding relative variations (in analogy to Krassovsky's ratio) is 7.7, which is in the range of observations of Krassovsky's ratio published for periodic oscillations. So, this shows how the brightness change is much more conspicuous than the (dynamically) corresponding temperature effect. The next case (panel b) turns out to be the strongest ABJ of all, with 125%, which lasts 30 min. The multiple ABJs including rapid successions of positive and negative jumps (c) vary between 38% and 63% with durations from 5 to 15 min. Another example of multiple ABJs, but involving only a sequence of brightness drops (d) of approximately median duration and strength, also shows correlated temperature variations. The ABJ of panel e, towards the end of the night in O_2 brightness (without affecting the OH layer), is another case of median strength.

An ABJ simultaneously present in OH and O_2 brightness (panel f, at about 3:30 UT) shows features typical of literature reports on mesospheric bores: the relatively fast rise in OH brightness (10 min) is accompanied by a drop in O_2 brightness followed by some rapidly decaying oscillations (like an "undular bore").

The temporal structure of another ABJ with about median characteristics (57% in 16.3 min) is shown time-resolved in Fig. 2, including error bars of the individual measurements. The nearly linear decay in OH brightness that ends abruptly at 8:00 UT is well documented by a dozen data points. Note that the error bars, which contain a contribution from the errors in rotational temperature due to the extrapolation from spectral samples to band intensity, have negligible effect on the interpretation of the phenomenon.

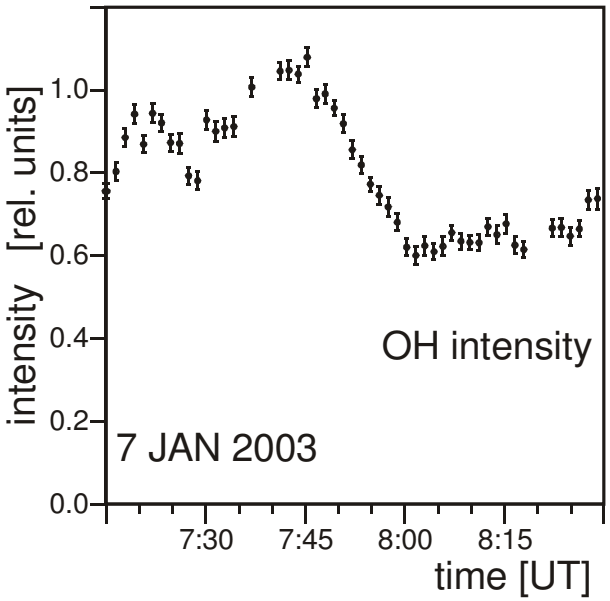

Fig. 2. Fine structure of an ABJ of typical strength. Individual data points are shown with error bars. Intensity units are normalized by the long-term mean, as in Fig. 1.

To put the quantitative characteristics of the complete set of ABJs into perspective, we compare with the classical ALOHA-93 bore event in terms of our strength and duration notation. The bore observed by Taylor et al. (1995) had an OH intensity variation of about 63% in 7 min, placing it into the upper half of our rankings. The El Leoncito bore event of 23 August 2001 (Smith et al., 2006), which is of course included in our list of ABJs, had an OH brightness variation of 68% in 11 min.

On the other hand, normal gravity waves detected with airglow imagers have much lower amplitudes, although statistical information on this is rarely reported. A recent exception is the paper by Suzuki et al. (2009), which shows the brightness amplitude distribution of over 700 gravity wave events detected in OH airglow. The amplitudes of these waves can be expressed as peak-to-peak values to become consistent with our strength definition. According to Fig. 2 of the paper by Suzuki et al. (2009),

nearly half of the gravity waves have peak-to-peak amplitudes below 2%, which is therefore the median strength. On the other hand, the median ABJ strength of 52% is about 25 times higher. There is also a considerable difference between the most intense gravity waves and the weakest ABJs. About 90% of the gravity waves have peak-to-peak amplitudes below 6% (and none has more than 14%), while the strength of the weakest ABJ is 22%.

3. Results

Although some nights contain more than one ABJ event, the following statistics will be mainly based on the number of nights with ABJs (independent of the timing of individual ABJ events, which will only be used to determine the hourly distribution). This makes sense on the assumption that the geophysical conditions favourable for the formation of ABJs are long-lived enough so that multiple ABJ observations in a single night only add confirmative redundance to the identification as ABJ night. We will see below that the assumption is supported by the results. The monthly number of ABJ nights in the different years is given in Table 2. The total number of 132 ABJ nights among the 2187 data nights means that, on average, 6.0% of the nights show ABJ events. Not all the years yield the same mean proportion, but the fluctuations are generally not very strong. Except for 1988 and 1997 (1988 had 2 events in 5 nights of observation, and 1997 not a single event in 72 nights), the percentage of ABJ nights varies between 3% and 9.4%. However, even the stronger variations in the years with better statistics seem to be only normal statistical fluctuations.

Table 2: Monthly and year-to-year distribution of nights with ABJ events, including the numbers of ABJ nights per year and per month. The last two columns show the total number of nights (from Table 1), and the percentage of nights with ABJs.

year	jan	feb	mar	apr	may	jun	jul	aug	sep	oct	nov	dec	sum	obs	%ABJ
1986						1	1			1			3	35	9
1987									1				1	17	6
1988												2	2	5	40
1992										1			1	16	6
1997														72	0
1998	1				4	5	5	1			2		18	192	9.4
1999		1		1		3	1						6	201	3
2000	1			1		3	3	1					9	226	4
2001					3			6	1		1	2	13	197	6.6
2002	1			1	2	5	3	2	1	1		1	17	280	6.1
2003	1												1	12	8
2006			1	2	3	5	4	1	1	4	3	2	26	287	9.1
2007			1		1	3	1	1		1	1	2	11	311	3.5
2008	3	2		2	2	3	2	1	1	4	2	2	24	336	7.1
sum	7	3	2	7	15	28	20	13	5	12	9	11	132	2187	6.0

The manifestation of ABJs in the different airglow layers is rather different. In contrast to what one could expect from the mesospheric bores reported in the literature, only a small fraction of the 132 ABJ nights involve both airglow emissions: ABJs in both layers occur in 18 nights. Also surprisingly, most nights

(namely, 80) show ABJ signatures only in the OH layer, while 34 nights have ABJ activity only in the O_2 layer.

For the 80 nights involving the OH emission alone, the monthly distribution is shown in Fig. 3a. The most striking features are a dominant peak in June, the absence of cases in February and March, the minimum in September, and the broad but flat distribution from November to January. A more robust quantification results from binning over four months: when we divide the year equally into three four-month seasons, namely the winter interval from May to August, the summer months from November to February, and the "equinox months" March, April, September, and October, we find that 56 ABJ nights belong to the winter interval, 15 to summer months, and only 9 correspond to equinox.

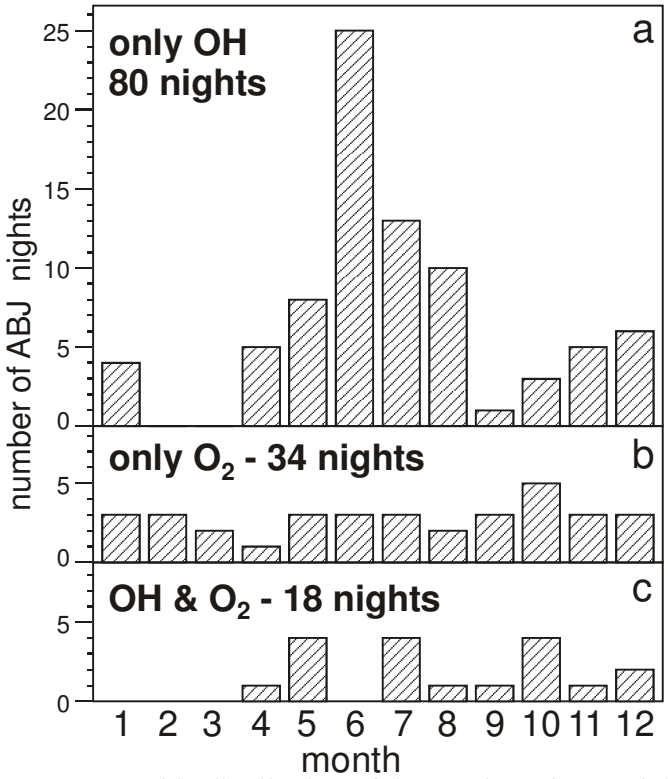

Fig. 3. Monthly distribution of the number of ABJ nights, observed only in the OH emission (a), only in the O_2 emission (b), and in both emissions during the same night (c).

The geophysical interpretation of Fig. 3a would not change essentially if the monthly distribution of available data (as given in Table 1) is taken into account. From the absolute numbers, the occurrence probability in each four-month period is obtained from division by the number of observation nights. That is, we arrive at the result that 7.1% of the nights have OH-only ABJ events in winter, 2.5% in summer, and only 1.1%, around equinox. To diminish the bias due to the seasonal variation of night duration, we can alternatively normalize by the total hours of effective observation, which gives 8.1, 3.9, and 1.4 ABJ nights per 1000 hours of observation, respectively

(see Table 3). So, both variants transmit a similar message: ABJ nights are 2 to nearly 3 times more likely to occur in winter than in summer. In the equinox months, the probability of ABJ nights is smallest, namely about six times smaller than in winter.

Table 3: Overview of number and occurrence frequency of nights with ABJs observed only in the OH emission, for three 4-month seasons, percentage of data nights with ABJs, total number of observation hours, and number of ABJ nights per 1000 hours of observation.

season	ABJ nights	%ABJ	obs. hours	ABJ/1000h
May–Aug	56	7.1	6879	8.14
Nov–Feb	15	2.5	3821	3.93
Mar Apr Sep Oct	9	1.1	6435	1.40

This monthly distribution of ABJ nights (involving only the OH emission) was used to verify statistical homogeneity of the ABJ list. We have tentatively divided the list of ABJ events into two halves, according to whether the rate of variation falls above or below the median value. The OH ABJ distribution was found to be quite similar for the two populations. This means that the statistics does not deteriorate by including the cases with slower variation, and it is legitimate to work with the complete set of data.

In striking contrast to the strong seasonal modulation seen in the OH-only case, the distribution of the 34 nights with events only present in O_2 is almost completely flat (see Fig. 3b). Or, expressed in terms of the 4-month seasons, there are 11 winter, 12 summer, and 11 equinox ABJ nights. The corresponding occurrence probability (based on nights, or hours of observations) would show some modulation, but now in the opposite sense of the OH-only distribution, that is, favouring summer instead of winter. At any rate, the deviation from isotropy is not very strong.

As mentioned, there are 18 additional nights with ABJs in both emission layers. They appear irregularly scattered over the months, without suggesting any geophysically meaningful pattern (see Fig. 3c). During 16 nights in this class, the OH and O_2 events occur at the same time (more precisely, they have temporal overlap) so that they are likely to be part of the same phenomenon. Of these, 14 are anticorrelated, that is, while the intensity grows in one emission, it decreases in the other one. In 2 nights both emissions vary in the same sense (of decreasing brightness).

Another important result may be referred to as "clustering": a considerable fraction of the ABJ nights (42 of 132) are part of 18 runs of consecutive, or nearly consecutive, nights (eventually separated by one or two nights without detected ABJ events). 15 of these clusters occur in May to August, and only one each in January, April, and November. All clusters involve OH, of which seven also involve O_2. While 7 of the clusters are only documented by 2 neighbouring ABJ nights, the 11 other cases are runs of 3 to 6 nights. The longest run of consecutive ABJ nights was

from 1 to 4 July 1998, the longest spans (including gaps) were 18, 21, 23 May 2001, and 19, 21, 22, 24 June 2006.

We have verified that the number and characteristics of the observed clusters are not just due to chance, by means of a statistical model assuming a contiguous dataset, and constant occurrence probability of ABJ nights. The expectation for the number of runs with lengths between 2 and 6 was determined from a binomial distribution bordered by two ABJ nights. Briefly (to avoid lengthy explanations about how to deal with short runs appearing as subsets of longer ones, the effect of data gaps, and other technical details), we just state that the model clearly underestimates the number of observed cases. This clustering then calls for a geophysical explanation. It means that conditions favouring the formation of ABJs prevail for several days.

Among our 132 ABJ nights, there are also 12 where an intensity rise is more or less immediately followed by a similar decrease, or vice versa, as the examples in Fig. 3c. OH intensity is involved in 9 nights, while 5 nights involve O_2. These events may be "solitary pulses" as those reported by Bageston et al. (2009). Because of the very strong amplitudes, it is highly unlikely that these pulses are due to the linear superposition of (several) normal gravity waves.

The local time distribution of our ABJ events is practically isotropic. The number of cases in 2-hourly bins (starting at 23:00 UT) is 29, 36, 38, 36, 30 (the decay in the first and last bins is a dusk/dawn effect). There are 95 events before, and 81 after local midnight. This is in contrast to the findings at the equatorial site São João do Cariri (7.5°S, 36.5°W), where airglow imager data led to the detection of 64 bore events over 226 nights of observation (Fechine et al., 2005). These authors reported a strong pre-midnight concentration of bore events (by 80%).

4. Discussion

The available evidence suggests that the set of ABJ events presented is reasonably well defined. We do not assume that ABJs represent a new phenomenon, but consider them to be manifestations of nonlinear waves like wall or bore events. In the present context, it is not helpful to discriminate between the different types of nonlinear waves. On the other hand, the concept of a duct as a necessary condition for the existence of nonlinear waves (e.g., Dewan and Picard, 1998; Seyler, 2005; Laughman et al., 2009) is useful for understanding some of our findings.

The relation between ABJs and nonlinear waves was investigated for two nights when our instrument saw ABJs in the OH emission while the Boston University imager registered the spatial development of the large-scale front events (Smith et al. 2006). A complete survey of the imager data, and the extension of the present

analysis to include the most recent data, might produce more opportunities to verify the nonlinear nature of ABJs.

The fact that 61% of the ABJ nights do not involve the higher airglow layer, but only OH, may have to do with duct altitude. This result may mean that ducts would tend to appear more frequently at lower altitudes. The only publication (which we are aware of) that supports a similar view for the mesopause region is the paper by Medeiros et al. (2005). Their conclusion was based on the comparison of the bore signatures simultaneously observed in OH, O_2, and OI 5577 (from a layer assumed to be 2 km higher than O_2) airglow, and not on cases limited to one airglow emission.

The strong seasonal modulation in the occurrence of the OH-only ABJ nights may be related to earlier findings at lower mesospheric heights by Hauchecorne et al. (1987). Their Rayleigh lidar results from 44°N showed that the probability of mesospheric inversion layers (which are candidates for ducting conditions) also peaks in winter, has a secondary maximum in summer, and minima around equinox. Note that this lidar result refers to any altitude between 55 and 83 km, below the mesopause region.

Hauchecorne et al. (1987) also discussed a relation between the seasonal variation in the probability of mesospheric inversion layers and the semiannual variation of gravity wave activity. Our previous results on the seasonal variation of gravity wave activity deduced from the El Leoncito OH airglow data (Reisin and Scheer, 2004) are indeed consistent with the main features of the OH ABJ distribution of Fig. 3a. This would seem to support the mechanisms discussed by Hauchecorne et al. (1987). However, since the gravity wave activity in the O_2 layer (Reisin and Scheer, 2004) has essentially the same seasonal variation as the OH layer, while the occurrence of ABJ nights involving O_2 (Fig. 3b) is completely different, the situation at 95 km does not easily fit into this scheme.

Apart from gravity wave activity, the seasonal behaviour of other parameters observed at El Leoncito (with winter maximum and equinox minima) is also similar to the OH ABJ distribution. This is the case for mean OH temperatures and brightness (Reisin and Scheer, 2009) and the seasonal occurrence of bright nights in OH (called airglow "bursts" in Scheer et al., 2005). These bright-night bursts are strongly associated with quasi-monochromatic gravity waves (Scheer and Reisin, 2002; Scheer et al., 2005). Quasi-monochromatic gravity waves are indicative of ducts (Walterscheid et al., 1999), as nonlinear waves are. One might therefore expect a narrow relationship between the occurrence of these bursts and ABJ nights, in spite of the different time scales involved in both phenomena. However, a detailed comparison of the dates when ABJs and bursts occur shows nearly no overlap: Only 3 of the 98 ABJ nights involving OH are also OH bursts (from a total of 25 OH bursts), and something similar holds for the O_2 emission (3 cases out of 52 O_2 ABJ nights and 43 O_2 bursts). This suggests that ABJs and airglow bursts are not narrowly

related and do require different geophysical conditions. Similarities of seasonal shape can be misleading.

In the case of ABJs limited to the O_2 emission, the contrast to the seasonal variations of mean O_2 temperatures and brightness, and the occurrence of O_2 airglow bursts is very strong. The nearly complete flatness of the O_2 ABJ histogram (Fig. 3b) suggests no plausible relation to the pronounced seasonal modulations in the other parameters which peak in April (Reisin and Scheer, 2009; Scheer et al., 2005). This behaviour does not give a clue to any simple geophysical explanation.

The relative scarcity of our ABJ events in both emissions can be explained by the smaller probability of a duct to affect the two emission layers, if the duct is not much wider than the layer separation (as is usually assumed). The probability obviously depends on the vertical position of the duct with respect to the airglow layers. Among the two-emission cases, the preponderance of anticorrelated brightness change (in 14 of 16 nights with simultaneous ABJs) in both emissions agrees with the typical situation observed for bore events. This is also a feature of the bore models if the symmetry plane of the duct falls between the airglow layers. A little more than half of the 64 bore events analyzed by Medeiros et al. (2005) showed such an anticorrelation between OH and O_2 (34 cases; according to Fig. 3 of that paper, this is the sum of the events labelled BDD, DBB, and "others"), while the rest was correlated. Our 2 correlated cases may simply be due to an unusually large vertical extension of the duct with a vertical position so that both airglow layers are on the same side of its symmetry plane. Of course, the width of the airglow layers (comparable to duct width) would have to be taken into account to model the effect of bores on airglow brightness more precisely.

The observed clustering into (near) consecutive runs of ABJ nights looks reasonable in the light of the earlier finding by Hauchecorne et al. (1987) of temperature inversion layers frequently persisting for several (typically five) days. Note that those authors find inversion layers also in heights where airglow data are not available, so that there may be nonlinear waves in the atmosphere that remain unobservable, but are possibly even more common than in the mesopause region. We note that Dewan and Picard (2001) had already interpreted the findings of Hauchecorne et al. (1987) in this sense.

5. Conclusions

The present analysis has led to the following conclusions. From a total of 2187 nights of airglow data, 132 nights (i.e., 6%) show strong and fast ABJs. Most of these (80) are limited to the OH layer. Only 34 (26%) exclusively involve the O_2 emission, and even less (16, or 12%) show simultaneous ABJs in both emissions.

That simultaneous ABJs in both emissions should be less frequent than those only visible in O_2 may be related to the vertical position and limited extension of the corresponding duct (believed to be a necessary condition for the formation of nonlinear waves). Most of the nights with simultaneous ABJs show an increase of one emission accompanied by a decrease of the other emission. Such an anticorrelation has often been reported in the literature about "wall events" and "tidal bores".

The ABJs that affect only the OH layer show a very pronounced seasonal variation, with a (southern) winter maximum centered around solstice (June), minima in March and September, and shallow low level throughout summer (at less than half of the winter probability). This seasonal distribution is not reproduced for nights with ABJs only in the O_2 emission, which is essentially uniform. A relation to gravity wave activity is likely for the OH layer, but not the dominant factor for the O_2 layer.

About 32% of the ABJ nights belong to runs of (nearly) consecutive nights with a maximum length of six nights. This clustering seems to be a consequence of the typical life time of ducting conditions.

In general, ABJ nights do not coincide with bright nights, in contrast to what might be expected from the relation with ducts (the relation is indirect, for bright nights).

In disagreement with the pre-midnight concentration of mesospheric bores observed at an equatorial site, we find a uniform local time distribution of ABJs. This may be due to geographical differences in wave sources.

Acknowledgements

The authors dedicate this paper to the memory of Edmond M. Dewan. We thank the Director and staff of CASLEO for technical support, and especially J.L. Aballay, J.L. Giuliani, R. Godoy, and J.D. Pinto, for often resolving problems with our instrument. This work was partially funded through CONICET PIP 112-200801-00287 and ANPCyT PICT 33370/2005 grants.

References

Bageston, J.V., Wrasse, C.M., Gobbi, D., Takahashi, H., Souza, P.B., 2009. Observation of mesospheric gravity waves at Comandante Ferraz Antarctica Station (62°S). Annales Geophysicae 27, 2593-2598.

Brown, L.B., Gerrard, A.J., Meriwether, J.W., Makela, J.J., 2004. All-sky imaging observations of mesospheric fronts in OI 557.7 nm and broadband OH airglow emissions: Analysis of frontal structure, atmospheric background conditions, and potential sourcing mechanisms. Journal of Geophysical Research 109, D19104, doi:10.1029/2003JD004223.

Dewan, E.M., Picard, R.H., 1998. Mesospheric bores. Journal of Geophysical Research 103, 6295-6305.

Dewan, E.M., Picard, R.H., 2001. On the origin of mesospheric bores. Journal of Geophysical Research 106, 2921-2927.

Drazin, P.G., Johnson, R.S., 1993. Solitons: an introduction. Cambridge University Press, Cambridge UK.

Fechine, J., Medeiros, A.F., Buriti, R.A., Takahashi, H., Gobbi, D., 2005. Mesospheric bore events in the equatorial middle atmosphere. Journal of Atmospheric and Solar-Terrestrial Physics 67(17-18), 1774-1778.

Fechine, J., Wrasse, C.M., Takahashi, H., Medeiros, A.F., Batista, P.P., Clemesha, B.R., Lima, L.M., Fritts, D., Laughman, B., Taylor, M.J., Pautet, P.D., Mlynczak, M.G., Russell, J.M., 2009. First observation of an undular mesospheric bore in a Doppler duct. Annales Geophysicae 27, 1399-1406.

Hauchecorne, A., Chanin, M.L., Wilson, R., 1987. Mesospheric temperature inversion and gravity wave breaking. Geophysical Research Letters 14(9), 933-936.

Laughman, B., Fritts, D.C., Werne, J., 2009. Numerical simulation of bore generation and morphology in thermal and Doppler ducts. Annales Geophysicae 27, 511-523.

Li, F., Swenson, G.R., Liu, A.Z., Taylor, M., Zhao, Y., 2007. Investigation of a "wall" wave event. Journal of Geophysical Research 112(D4), D04104, doi:10.1029/2006JD007213.

Liu, A.Z., Swenson, G.R., 2003. A modeling study of O_2 and OH airglow perturbations induced by atmospheric gravity waves. Journal of Geophysical Research 108, doi:10.1029/2002JD002474.

Medeiros, A.F., Fechine, J., Buriti, R.A., Takahashi, H., Wrasse, C.M., Gobbi, D., 2005. Response of OH, O_2 and OI5577 airglow emissions to the mesospheric bore in the equatorial region of Brazil. Advances in Space Research 35(11), 1971-1975.

Mobbs, S.D., 1985. Propagation of nonlinear internal gravity waves at stratospheric and mesospheric heights. III: The wave shape. Annales Geophysicae 3(5), 599-608.

Nielsen, K., Taylor, M.J., Stockwell, R.G., Jarvis, M.J., 2006. An unusual mesospheric bore event observed at high latitudes over Antarctica. Geophysical Research Letters 33(7), L07803, doi:10.1029/2005GL025649.

Reisin, E.R., Scheer, J., 1996. Characteristics of atmospheric waves in the tidal period range derived from zenith observations of O_2(0-1) Atmospheric and OH(6-2) airglow at lower midlatitudes. Journal of Geophysical Research 101, 21223-21232.

Reisin, E.R., Scheer, J., 2001. Vertical propagation of gravity waves determined from zenith observations of airglow. Advances in Space Research 27(10), 1743-1748.

Reisin, E.R., Scheer, J., 2004. Gravity wave activity in the mesopause region from airglow measurements at El Leoncito. Journal of Atmospheric and Solar-Terrestrial Physics 66(6-9), 655-661.

Reisin, E.R., Scheer, J., 2009. Evidence of change after 2001 in the seasonal behaviour of the mesopause region from airglow data at El Leoncito. Advances in Space Research 44(3), 401-412.

Scheer, J., Reisin, E.R., 2001. Refinements of a classical technique of airglow spectroscopy. Advances in Space Research 27(6-7), 1153-1158.

Scheer, J., Reisin, E.R., 2002. Most prominent airglow night at El Leoncito. Journal of Atmospheric and Solar-Terrestrial Physics 64(8-11), 1175-1181.

Scheer, J., Reisin, E.R., Batista, P.P., Clemesha, B.R., Takahashi, H., 2005. Detection of meteor radar wind signatures related to strong short-duration day-to-day airglow transitions at sites 2600 km apart. Journal of Atmospheric and Solar-Terrestrial Physics 67(6), 611-621.

Seyler, C.E., 2005. Internal waves and undular bores in mesospheric inversion layers. Journal of Geophysical Research 110, D09S05, doi:10.10129/2004JD004685.

She, C.Y., Li, T., Williams, B.P., Yuan, T., Picard, R.H., 2004. Concurrent OH imager and sodium temperature/wind lidar observation of a mesopause region undular bore event over Fort Collins/Platteville, Colorado. Journal of Geophysical Research 109, D22107, doi:10.1029/2004JD004742.

Shiokawa, K., Suzuki, S., Otsuka, Y., Ogawa, T., Nakamura, T., Mlynczak, M.G., Russell III, J.M., 2006. A multi-instrument measurement of a mesospheric front-like structure at the equator. Journal of the Meteorological Society of Japan 84A, 305-316.

Smith, S.M., Taylor, M.J., Swenson, G.R., She, C.-Y., Hocking, W., Baumgardner, J., Mendillo, M., 2003. A multi-diagnostic investigation of the mesospheric bore phenomenon. Journal of Geophysical Research 108 (A2), 1083, doi:10.1029/2002JA009500.

Smith, S.M., Friedman, J., Raizada, S., Tepley, C., Baumgardner, J., Mendillo, M., 2005. Evidence of mesospheric bore formation from a breaking gravity wave event: simultaneous imaging and lidar measurements. Journal of Atmospheric and Solar-Terrestrial Physics 67(4), 345-356.

Smith, S.M., Scheer, J., Reisin, E.R., Baumgardner, J., Mendillo, M., 2006. Characterization of exceptionally strong mesospheric wave events using all-sky and zenith airglow observations. Journal of Geophysical Research 111(A9), A09309, doi:10.1029/2005JA011197.

Snively, J.B., Pasko, V.P., Taylor, M.J., Hocking, W.K., 2007. Doppler ducting of short-period gravity waves by midlatitude tidal wind structure. Journal of Geophysical Research 112, A03304, doi:10.1029/2006JA011895.

Suzuki, S., Shiokawa, K., Liu, A.Z., Otsuka, Y., Ogawa, T., Nakamura, T., 2009. Characteristics of equatorial gravity waves derived from mesospheric airglow imaging observations. Annales Geophysicae 27, 1625-1629.

Swenson, G.R., Gardner, C.S., 1998. Analytical models for the responses of the mesospheric OH* and Na layers to atmospheric gravity waves. Journal of Geophysical Research 103, 6271-6294.

Swenson, G.R., Qian, J., Plane, J.M.C., Espy, P.J., Taylor, M.J., Turnbull, D.N., Lowe, R.P., 1998. Dynamical and chemical aspects of the mesospheric Na "wall" event on October 9, 1993 during the Airborne Lidar and Observations of Hawaiian Airglow (ALOHA) campaign. Journal of Geophysical Research 103, 6361-6380.

Tarasick, D.W., Hines, C.O., 1990. The observable effects of gravity waves on airglow emissions. Planetary and Space Science 38, 1105-1119.

Taylor, M.J., Turnbull, D.N., Lowe, R.P., 1995. Spectrometric and imaging measurements of a spectacular gravity wave event observed during the ALOHA-93 campaign. Geophysical Research Letters 22, 2849-2852.

Walterscheid, R.L., Hecht, J.H., Vincent, R.A., Reid, I.M., Woithe, J., Hickey, M.P., 1999. Analysis and interpretation of airglow and radar observations of quasi-monochromatic gravity waves in the upper mesosphere and lower thermosphere over Adelaide, Australia (35°S, 138°E). Journal of Atmospheric and Solar-Terrestrial Physics 61, 461-478.

Yue, J., She, C.-Y., Nakamura, T., Harrell, S., Yuan, T., 2009. Mesospheric bore formation from large-scale gravity wave perturbations observed by collocated all-sky OH imager and sodium lidar. Journal of Atmospheric and Solar-Terrestrial Physics 72(1), 7-18, doi:10.1016/j.jastp.2009.10.002.